Available online at www.sciencedirect.com
ScienceDirect
Icarus 195 (2008) 758–764
ICARUS
www.elsevier.com/locate/icarus

A model for the temperature-dependence of tidal dissipation in convective plumes on icy satellites: Implications for Europa and Enceladus

Giuseppe Mitri [a,*], Adam P. Showman [b]

[a] *Jet Propulsion Laboratory, California Institute of Technology, M/S 183-501, 4800 Oak Grove Drive, Pasadena, CA 91109, USA*
[b] *Department of Planetary Sciences and Lunar and Planetary Laboratory, University of Arizona, 1629 E. University Blvd., Tucson, AZ 85721, USA*

Received 26 July 2007; revised 10 January 2008

Available online 21 February 2008

Abstract

To explain the formation of surface features on Europa, Enceladus, and other satellites, many authors have postulated the spatial localization of tidal heating within convective plumes. However, the concept that enhanced tidal heating can occur within a convective plume has not been rigorously tested. Most models of this phenomenon adopt a tidal heating with a temperature-dependence derived for an incompressible, homogeneous (zero-dimensional) Maxwell material, but it is unclear whether this formulation is relevant to the heterogeneous situation of a warm plume surrounded by cold ice. To determine whether concentrated dissipation can occur in convective plumes, we develop a two-dimensional model to compute the volumetric dissipation rate for an idealized, vertically oriented, isolated convective plume obeying a Maxwellian viscoelastic compressible rheology. We apply the model to the Europa and Enceladus ice shells, and we investigate the consequences for partial melting and resurfacing processes on these bodies. We find that the tidal heating is strongly temperature dependent in a convective ice plume and could produce elevated temperatures and local partial melting in the ice shells of Europa and Enceladus. Our calculation provides the first quantitative verification of the hypothesis by Sotin et al. [Sotin, C., Head, J.W., Tobie, G., 2002. Geophys. Res. Lett. 29. 74-1] and others that the tidal dissipation rate is a strong function of temperature inside a convective plume. On Europa, such localized heating could help allow the formation of domes and chaos terrains by convection. On Enceladus, localized tidal heating in a thermal plume could explain the concentrated activity at the south pole and its associated heat transport of 2–7 GW.

Keywords: Enceladus; Europa; Geophysics; Ices; Interiors; Jupiter, satellites; Saturn, satellites

1. Introduction

To explain the formation of surface features on Europa, Enceladus, and other satellites, many authors have postulated the spatial localization of tidal heating within convective plumes. The pits, domes and chaotic terrains observed on Europa may have resulted from convective motions in the ice shell (Pappalardo et al., 1998; Nimmo and Manga, 2002; Showman and Han, 2004, 2005; Han and Showman, 2005) or melt-through of the ice shell (Greenberg et al., 1999; Thomson and Delaney, 2001; Melosh et al., 2004). Collins et al. (2000) proposed that chaos areas are formed over liquid deposits or partial melt within the ice shell. Sotin et al. (2002) argued that tidal dissipation might heat diapirs and produce melting at shallow depths within Europa' ice shell. Successively, under the assumption that tidal heating depends strongly on local temperature in a heterogeneous ice shell, Tobie et al. (2003) have shown that tidal dissipation can heat the thermal plume to the melting temperature, with consequent episodic upwelling of partially molten ice. If the mean tidal heating is sufficiently strong, hot thermal plumes are more likely to experience melting than the background ice simply because they are slightly (∼10 K) closer to the melting temperature (e.g., Tobie et al., 2003). However, without localization of the *tidal heating*, this process can only localize *partial melting* in the hot plumes for carefully tuned values of the tidal heating rates—modestly larger tidal heating rates, for example, would lead to widespread melting throughout the ice shell. In contrast, spatially concentrated tidal heating is an attractive and

* Corresponding author. Fax: +1 818 354 0966.
E-mail address: giuseppe.mitri@jpl.nasa.gov (G. Mitri).

0019-1035/$ – see front matter
doi:10.1016/j.icarus.2008.01.010

commonly invoked mechanism for naturally inducing localized heating and partial melting within plumes (Sotin et al., 2002; Tobie et al., 2003).

The Imaging Science Subsystem (ISS) on board the Cassini spacecraft has shown that the south pole of Saturn's satellite Enceladus is geologically active (Porco et al., 2006). Cassini Composite Infrared Spectrometer (CIRS) data show that the south polar regions are warmer (between 114 and 157 K) (Spencer et al., 2006) than surrounding regions (∼70–80 K). CIRS data suggest that the current thermal emission from the south polar terrains is 3 to 7 GW (Spencer et al., 2006). A plume of water vapor and small icy particles has been observed at the south polar regions (Spahn et al., 2006; Waite et al., 2006). Porco et al. (2006) proposed that subsurface reservoirs of liquid can erupt through vents and produce the observed plumes. Moreover, Porco et al. suggested that the processes producing the observed heating might result in local regions with higher temperatures, leading to subsurface reservoir of liquid water. Likewise, an ascending diapir, perhaps aided by localized tidal heating, may help explain the active south polar regions of Enceladus (Nimmo and Pappalardo, 2006).

However, the hypothesis that enhanced tidal heating can occur within a convective plume has not been rigorously tested. To date, models of tidal heating in heterogeneous systems have focused primarily on shear heating along pre-existing linear fractures (Gaidos and Nimmo, 2000; Nimmo and Gaidos, 2002; Nimmo et al., 2007). In this scenario, the lithosphere is divided into two mechanically distinct plates by the fracture. This mechanical separation into two distinct plates implies that if the fracture zone is sufficiently weaker than the surrounding ice, the tidal deformation (and hence the tidal heating) can focus almost completely along the fracture, with minimal deformation occurring in the plates themselves. Because warmer ice is softer, this promotes a strong positive feedback, wherein enhanced tidal heating along the fracture leads to increased temperature, further weakening (i.e., decreased viscosity), and hence runaway increases in tidal heating along the fracture.

In contrast, warm, ascending convective plumes are surrounded on all sides by colder, stiffer ice. Because of this geometric confinement, the amplitude of total tidal deformation within a warm plume cannot become greatly enhanced within the plume as it can along a fracture separating two distinct plates. Thus, the positive feedback that enhances the tidal heating along pre-existing fractures (Nimmo and Gaidos, 2002) is ruled out for a convective plume. Indeed, linear elastic calculations of a stressed mechanical plate containing a circular hole show that the stress becomes enhanced by only a factor of several at the edge of the hole (Mal and Singh, 1991, p. 221). This argument hints that, analogously, a convective plume with a circular cross-section might have a rate of tidal dissipation enhanced by only a factor of several relative to the surrounding ice. However, in an ice shell subjected to cyclical tidal stress, the tidal heating rate is determined not only by the absolute *amplitude* of tidal flexing and stress over a tidal cycle but by the *phase shift* between the cyclically varying stress and strain rate. One must therefore solve the full viscoelastic problem to determine whether dissipation in a convective plume becomes enhanced relative to that in the surroundings.

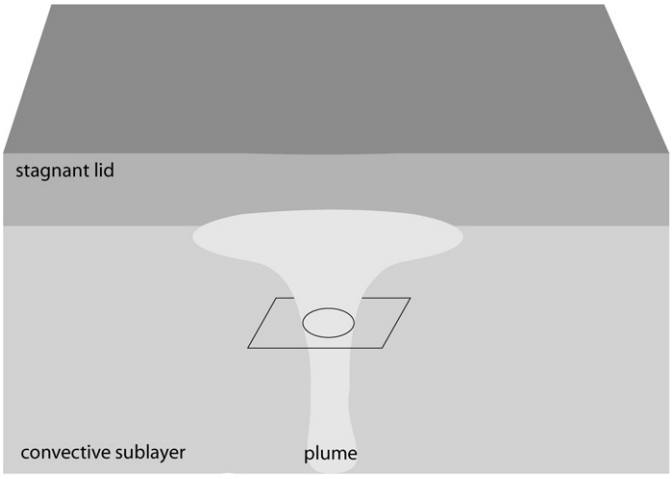

Fig. 1. The model examines a two-dimensional horizontal section of a convective ice shell representing a cross section through a vertically oriented convective plume.

Despite the lack of definitive calculations clarifying this issue, most authors of icy-satellite convection papers have simply *assumed* that the tidal heating rate is strongly dependent on the local temperature according to the predictions of the incompressible, homogeneous (zero-dimensional) Maxwell material (Wang and Stevenson, 2000; Sotin et al., 2002; Tobie et al., 2003; Showman and Han, 2004; Mitri and Showman, 2005). This zero-dimensional model generally predicts a maximum of dissipation for flexing periods $\omega^{-1} \approx \eta/\mu$, where ω is the frequency of the tidal flexing of the ice shell and η and μ are the viscosity and the shear modulus of the ice, respectively. However, it is unclear whether this formulation is relevant to the heterogeneous situation of a warm plume surrounded by cold ice.

To determine whether concentrated dissipation can occur in convective plumes, we develop a two-dimensional model to compute the volumetric dissipation rate for a Maxwellian viscoelastic compressible material. We apply the model to Europa and Enceladus and investigate the consequences for partial melting and resurfacing processes on these bodies.

2. Model

The model examines a two-dimensional horizontal section of a convective ice shell representing a cross section through a vertically oriented convective plume (Fig. 1). In this geometry, the cross section through an upwelling (or a downwelling) in the ice shell is represented as a disk. The disk is embedded in an unbounded material (matrix). Although convective systems generally contain multiple plumes, high-Rayleigh number convection simulations show that plumes widths are generally much smaller than the distance between plumes, so it is reasonable to proceed by considering an isolated plume. While this is probably a better assumption for Europa than Enceladus, several authors have advanced the hypothesis that a regionalized hot thermal plume or diaper may reside un-

derneath Enceladus' south polar terrains (Grott et al., 2007; Nimmo and Pappalardo, 2006). We specify the imposed, oscillatory tidal stress field as a boundary condition at infinity, and solve for the stresses and strains throughout the domain. This allows us to calculate the tidal dissipation within and around the plume.

With these assumptions, the problem becomes mathematically equivalent to the classic elastic inclusion problem, the solution for which is well known (Mal and Singh, 1991, p. 221).

2.1. Boundary conditions

We solve the inclusion problem for a plane Maxwellian viscoelastic compressible material with Newtonian rheology. The interface between the matrix and the disk is welded. At the interface between the disk and the surrounding matrix, the displacement and stress are continuous. The coordinate system is oriented such that, at $r \to \infty$, the imposed tidal stress is represented as the boundary condition $\sigma_{xx}(r \to \infty) = \sigma_0$ with $\sigma_{yy}(r \to \infty) = 0$, where r is the radial distance from the center of the disk and σ_{xx} and σ_{yy} are the normal stresses in a Cartesian coordinate system with axes x and y. Using standard coordinate transformations (Jaeger and Cook 1979, pp. 13, 50), we represent this boundary condition at $r \to \infty$ in cylindrical coordinates:

$$\sigma_{rr}^{\text{mat}} = \frac{\sigma_0}{2}(1 + \cos 2\varphi), \tag{1}$$

$$\sigma_{\varphi\varphi}^{\text{mat}} = \frac{\sigma_0}{2}(1 - \cos 2\varphi), \tag{2}$$

$$\sigma_{r\varphi}^{\text{mat}} = -\frac{\sigma_0}{2}\sin 2\varphi, \tag{3}$$

where the tensor indices in polar coordinates are r and φ, where r is the radial distance from the center of the disk and φ is the angle from the x axis.

2.2. Solution method: Equivalence between viscoelastic and elastic problems

We show that the viscoelastic problem we wish to solve is mathematically equivalent to an elastic problem. For a viscoelastic body the stress-strain relation for a Newtonian rheology is given in Cartesian coordinates by

$$\dot{\sigma}_{ik} + \frac{\mu}{\eta}\sigma_{ik} = \frac{2\mu\nu}{1-2\nu}\dot{\varepsilon}_{jj}\delta_{ik} + 2\mu\dot{\varepsilon}_{ik}, \tag{4}$$

where the dot denotes the derivation in time t, σ_{ik} is the stress tensor, ε_{ik} is the strain tensor, δ_{ik} is the Kronecker delta, η is the viscosity, μ is the shear modulus, ν is Poisson's ratio, and i, j, k are tensorial indices.

The ice shell is subject to a periodic tidal flexing, represented as $\sigma_{ij} = \sigma_{ij}^0 e^{i\omega t}$, and $\varepsilon_{ij} = \varepsilon_{ij}^0 e^{i\omega t}$, where σ_{ij}^0 and ε_{ij}^0 are the complex amplitudes of the stress and strain tensors, respectively, ω is the orbital frequency, and in the exponent $i^2 = -1$. The stress-strain relation is reduced to

$$\sigma_{ik}^0 = \frac{2\tilde{\mu}\nu}{1-2\nu}\varepsilon_{jj}^0\delta_{ik} + 2\tilde{\mu}\varepsilon_{ik}^0, \tag{5}$$

where $\tilde{\mu}$ is a complex shear modulus ($\tilde{\mu} \in \mathbf{C}$) given by

$$\tilde{\mu} = \frac{\omega^2\mu\eta^2}{\mu^2 + \omega^2\eta^2} + i\frac{\omega\mu^2\eta}{\mu^2 + \omega^2\eta^2}. \tag{6}$$

Equation (5) is formally the stress-strain relation of a Hookean elastic body. Therefore, the solution of a viscoelastic problem for a body subjected to periodic stresses and strains corresponds to the solution of a Hookean elastic problem in the complex field with a shear modulus given by Eq. (6) (Biot, 1954). The known solution to the elastic inclusion problem (Mal and Singh, 1991, p. 221) therefore allows us to calculate σ_{ij}^0 and ε_{ij}^0 everywhere over the two-dimensional domain given assumptions about these quantities infinitely far from the plume.

2.3. Inclusion problem

Airy functions have been used to solve the inclusion problem. The adopted method is fully described in Mal and Singh (1991, p. 221). The displacement and stress components for an elastic inclusion problem are given by

$$u_r^{\text{mat}} = \frac{\sigma_0 r}{4\mu_{\text{mat}}}\left\{(2\alpha - 1) - \frac{1 + 2\alpha\beta - 2\alpha - \beta}{2\alpha + \beta - 1}\left(\frac{a}{r}\right)^2 + \left[1 + \frac{4\alpha(1-\beta)}{1 - \beta + 4\alpha\beta}\left(\frac{a}{r}\right)^2 - \frac{1-\beta}{1-\beta+4\alpha\beta}\left(\frac{a}{r}\right)^4\right]\cos 2\varphi\right\}, \tag{7}$$

$$u_\varphi^{\text{mat}} = \frac{\sigma_0 r}{4\mu_{\text{mat}}}\left[-1 + \frac{2(1-\beta)(1-2\alpha)}{1-\beta+4\alpha\beta}\left(\frac{a}{r}\right)^2 - \frac{1-\beta}{1-\beta+4\alpha\beta}\left(\frac{a}{r}\right)^4\right]\sin 2\varphi, \tag{8}$$

$$\sigma_{rr}^{\text{mat}} = \frac{\sigma_0}{2}\left\{1 + \frac{1 + 2\alpha\beta - 2\alpha - \beta}{2\alpha + \beta - 1}\left(\frac{a}{r}\right)^2 + \left[1 - \frac{4(1-\beta)}{1-\beta+4\alpha\beta}\left(\frac{a}{r}\right)^2 + \frac{3(1-\beta)}{1-\beta+4\alpha\beta}\left(\frac{a}{r}\right)^4\right]\cos 2\varphi\right\}, \tag{9}$$

$$\sigma_{\varphi\varphi}^{\text{mat}} = \frac{\sigma_0}{2}\left\{1 - \frac{1 + 2\alpha\beta - 2\alpha - \beta}{2\alpha + \beta - 1}\left(\frac{a}{r}\right)^2 - \left[1 + \frac{3(1-\beta)}{1-\beta+4\alpha\beta}\left(\frac{a}{r}\right)^4\right]\cos 2\varphi\right\}, \tag{10}$$

$$\sigma_{r\varphi}^{\text{mat}} = -\frac{\sigma_0}{2}\left[1 + \frac{2(1-\beta)}{1-\beta+4\alpha\beta}\left(\frac{a}{r}\right)^2 - \frac{3(1-\beta)}{1-\beta+4\alpha\beta}\left(\frac{a}{r}\right)^4\sin 2\varphi\right], \tag{11}$$

$$u_r^{\text{disk}} = \frac{\sigma_0\alpha\beta r}{2\mu_{\text{disk}}}\left(\frac{2\alpha - 1}{2\alpha + \beta - 1} + \frac{2\cos 2\varphi}{1 - \beta + 4\alpha\beta}\right), \tag{12}$$

$$u_\varphi^{\text{disk}} = -\frac{\sigma_0\alpha\beta r \sin 2\varphi}{\mu_{\text{disk}}(1 - \beta + 4\alpha\beta)}, \tag{13}$$

$$\sigma_{rr}^{\text{disk}} = \sigma_0\alpha\beta\left(\frac{1}{2\alpha+\beta-1}+\frac{2\cos 2\varphi}{1-\beta+4\alpha\beta}\right), \tag{14}$$

$$\sigma_{\varphi\varphi}^{\text{disk}} = \sigma_0\alpha\beta\left(\frac{1}{2\alpha+\beta-1}-\frac{2\cos 2\varphi}{1-\beta+4\alpha\beta}\right), \tag{15}$$

$$\sigma_{r\varphi}^{\text{disk}} = -\frac{2\sigma_0\alpha\beta\sin 2\varphi}{1-\beta+4\alpha\beta}, \tag{16}$$

where σ_0 is the amplitude of the imposed tidal stress at $r\to\infty$, a is the radius of the inclusion, and $\beta=\mu_{\text{disk}}/\mu_{\text{mat}}$, where μ_{disk} and μ_{mat} are the shear modulus of the disk and the matrix, respectively. The indices mat and disk denote the matrix and the disk, respectively. $\alpha=(1+\nu)^{-1}$ is for a plane strain problem and $\alpha=(1-\nu)$ is for a plane stress problem. The plane stress is for a stress state in which the normal stress, σ_{zz}, and the shear stress, σ_{xz} and σ_{yz}, are assumed to be zero. The plane strain is for a strain state in which the normal strain, ε_{zz}, and the shear strain, ε_{xz} and ε_{yz}, are assumed to be zero. We solve the problem for both plane strain and plane stress and we compare the results. For water ice where the Poisson's ratio is 0.314 we do not have significant difference between the two solutions of the problem ($\alpha=0.76$ for plane strain and $\alpha=0.69$ for plane stress).

We use the strain–displacement relations in cylindrical coordinates (e.g., Hetnarski and Ignaczak, 2004, p. 502)

$$\varepsilon_{rr}^{j} = \frac{\partial u_r^j}{\partial r}, \tag{17}$$

$$\varepsilon_{\varphi\varphi}^{j} = \frac{1}{r}\frac{\partial u_\varphi^j}{\partial\varphi}+\frac{u_r^j}{r}, \tag{18}$$

$$2\varepsilon_{r\varphi}^{j} = \frac{\partial u_\varphi^j}{\partial r}-\frac{u_\varphi^j}{r}+\frac{1}{r}\frac{\partial u_r^j}{\partial\varphi}, \tag{19}$$

where the indices j is for mat or disk.

2.4. Volumetric dissipation rate

Here we present the model to compute the volumetric dissipation rate of a Maxwellian compressible material subjected to periodic tension. See also the discussion on the volumetric dissipation rate in Tobie et al. (2005). The dissipation rate done by the forces $\frac{\partial\sigma_{ik}}{\partial x_k}$ per volume V, where x_k is a spatial coordinate, is

$$\int_V \sigma_{ik}\dot{\varepsilon}_{ik}\,\mathrm{d}^3x_k. \tag{20}$$

For the derivation of volumetric dissipation rate we can consider a dependence of the stress and strain rate tensors on time t as $e^{i\omega t}$

$$\sigma_{ik} = \mathrm{Re}\big[\sigma_{ik}^0 e^{i\omega t}\big] \equiv \frac{1}{2}\big[\sigma_{ik}^0 e^{i\omega t}+\sigma_{ik}^{0^*}e^{-i\omega t}\big], \tag{21}$$

$$\dot{\varepsilon}_{ik} = \mathrm{Re}\big[\dot{\varepsilon}_{ik}^0 e^{i\omega t}\big] \equiv \frac{1}{2}\big[\dot{\varepsilon}_{ik}^0 e^{i\omega t}+\dot{\varepsilon}_{ik}^{0^*}e^{-i\omega t}\big]. \tag{22}$$

We have used the relation $\mathrm{Re}[\Gamma]=(\Gamma+\Gamma^*)/2$, where Γ is a generic complex function. We adopt the convention to write $\mathrm{Re}[\Gamma]$ and $\mathrm{Im}[\Gamma]$ as the real part and the imaginary part of Γ, respectively. Then, the product of the stress and strain tensors is given by

$$\sigma_{ik}\dot{\varepsilon}_{ik} = \frac{1}{2}\mathrm{Re}\big[\sigma_{ik}^0\dot{\varepsilon}_{ik}^{0^*}+\sigma_{ik}^0\dot{\varepsilon}_{ik}^0 e^{2i\omega t}\big] \tag{23}$$

and the volumetric dissipation rate done in a cycle is

$$W = \frac{\omega}{2\pi}\oint\frac{1}{2}\mathrm{Re}\big[\sigma_{ik}^0\dot{\varepsilon}_{ik}^{0^*}+\sigma_{ik}^0\dot{\varepsilon}_{ik}^0 e^{2i\omega t}\big]\mathrm{d}t = \frac{1}{2}\mathrm{Re}\big[\sigma_{ik}^0\dot{\varepsilon}_{ik}^{0^*}\big]. \tag{24}$$

The contribution $\sigma_{ik}^0\dot{\varepsilon}_{ik}^0 e^{2i\omega t}$ in the cyclical integral is zero. Considering the dependence of the stress and strain rate tensors on $e^{i\omega t}$, and writing $\sigma_{ik}^0=\mathrm{Re}[\sigma_{ik}^0]+i\,\mathrm{Im}[\sigma_{ik}^0]$ and $\varepsilon_{ik}^0=\mathrm{Re}[\varepsilon_{ik}^0]+i\,\mathrm{Im}[\varepsilon_{ik}^0]$, Eq. (24) yields

$$W = \frac{\omega}{2}\big(\mathrm{Im}\big[\sigma_{ik}^0\big]\mathrm{Re}\big[\varepsilon_{ik}^0\big]-\mathrm{Re}\big[\sigma_{ik}^0\big]\mathrm{Im}\big[\varepsilon_{ik}^0\big]\big). \tag{25}$$

We convert the inclusion solution [Eqs. (7)–(16)] into Cartesian geometry and we compute the volumetric dissipation rate using Eq. (25). We compare the results obtained with the volumetric dissipation rate of a material with Poisson's ratio $\nu=0.5$.

2.5. Physical parameters

The Newtonian viscosity of the ice is given by (e.g., Mitri and Showman, 2005)

$$\eta = \eta_0\exp\left[A\left(\frac{T_{\text{ref}}}{T}-1\right)\right], \tag{26}$$

where η_0 is the ice viscosity at a temperature of 273 K ($10^{13}\leqslant\eta_0\leqslant 10^{15}$ Pa s), the constant $A=26$, corresponding to an activation energy of 60 kJ mol^{-1}, $T_{\text{ref}}=273$ K is a reference temperature and T is temperature. Equation (26) ignores premelting at ice-grain boundaries; this process can cause additional lowering of the viscosity close to the melting temperature. Most studies adopting a flow law analogous to Eq. (26) assume that T_{ref} is the pressure-dependent melting temperature of pure H_2O, leading to the so-called "homologous temperature" formulation in which the viscosity at the melting temperature in absence of ammonia equals η_0. However, as emphasized by (McKinnon, 2006), ice-rheology data do not support this assumption, and a constant value of T_{ref} (as adopted here) is equally consistent with the data.

The physical parameters used in the model are summarized in Table 1.

2.6. Tidal flexing of the ice shells

The tidal deformation of Europa from a spherical shape is given by (see Greenberg and Geissler, 2002)

$$d = h_2\left(\frac{3}{2}\cos^2\theta-\frac{1}{2}\right)\left[R_S\frac{M_P}{M_S}\left(\frac{R_S}{a}\right)^3\right], \tag{27}$$

where h_2 is the Love number, θ is the angular distance from Jupiter, M_P is the planet's mass, R_S is the satellite's radius, M_S is the satellite's mass, and a is the orbital semi-major axis. We adopt a Love number 1.2 for Europa (Greenberg and Geissler, 2002). The amplitude of the diurnal tidal flexing of the ice shell

Table 1
Physical parameters

Parameter	Symbol	Unit	Value
Radius, Europa	R_S	km	1565
Radius, Enceladus	R_S	km	252
Mass, Europa	M_S	kg	4.80×10^{22}
Mass, Enceladus	M_S	kg	1.08×10^{20}
Semi major axis, Europa	a	km	670,900
Semi major axis, Enceladus	a	km	238,020
Eccentricity, Europa	e		0.01
Eccentricity, Enceladus	e		0.0047
Orbital frequency, Europa	ω	s^{-1}	2.0×10^{-5}
Orbital frequency, Enceladus	ω	s^{-1}	5.3×10^{-5}
Love number, Europa	h_2		~1.2
Love number, Enceladus	h_2		0.01–0.2
Mass, Jupiter	M_P	kg	1.9×10^{27}
Mass, Saturn	M_P	kg	5.7×10^{26}
Poisson ratio	ν		0.314
Shear modulus	μ	Pa	4×10^9
Reference viscosity at 273 K	η_0	Pa s	10^{13}–10^{15}

is given by

$$\xi \sim 3ed, \tag{28}$$

where e is the orbital eccentricity. The diurnal tidal flexing of Europa ice shells is ~33 m. The ice shell tidal-flexing strain is, roughly, $\varepsilon_0 \sim \xi/R_S$ (Showman and Han, 2004; Mitri and Showman, 2005). Therefore, the tidal-flexing strain for Europa is $\sim 2 \times 10^{-5}$ (Ojakangas and Stevenson, 1989).

Nimmo et al. (2007) have considered that Enceladus ice shell is decoupled from the rocky interior by a liquid layer, implying that the Love number range between 0.01 and 0.2. Assuming that Eqs. (27) and (28) describe the amplitude of the diurnal tidal flexing of Enceladus, the strain amplitude ranges between 9×10^{-7} and 2×10^{-5}. The internal structure of Enceladus is not well constrained, and the tidal flexing of the ice shell might depend on factors that the simple model expressed with Eqs. (27) and (28) does not take into account. We therefore compute the volumetric dissipation rate of an isolated thermal plume for a large range of tidal-flexing amplitudes (10^{-7}–10^{-5}).

3. Results

Our calculation shows that the tidal heating is strongly temperature dependent in a convective plume. Fig. 2 shows the volumetric dissipation rate W within Europa's ice shell as a function of the distance r from the center of a plume (convective plume or diapir). This model assumes plane stress and adopts a tidal flexing strain 2×10^{-5}. The radius of the plume is 1 km and the reference viscosity of the ice is $\eta_0 = 10^{14}$ Pa s. The gray colored area in the plot represents a thermal plume in the ice shell, and we plot curves of the dissipation assuming a plume temperature of 250, 260, and 270 K (solid, dashed, and dotted, respectively). The white area shows the ice surrounding the thermal plume with a fixed temperature 250 K. As expected, the tidal dissipation far from the plume is independent of the plume temperature. The existence of the plume causes a slight

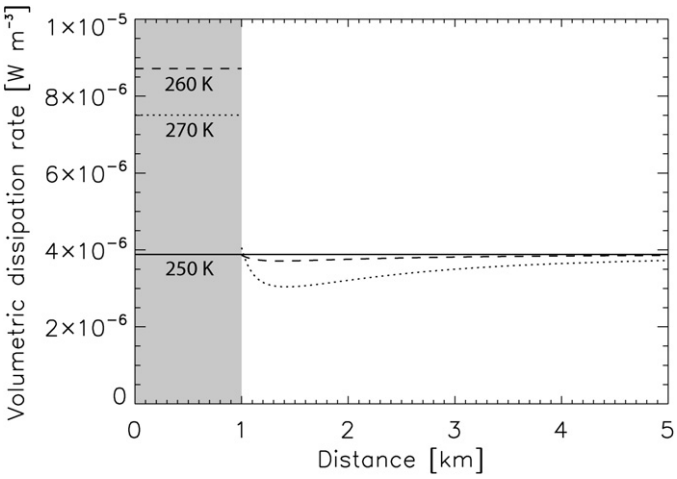

Fig. 2. Volumetric dissipation rate of the Europa ice shell as a function of distance from the center of a thermal plume. This model assumes a tidal flexing strain 2×10^{-5} and we solve the problem for plain stress. The radius of the plume is 1 km and the reference viscosity is $\eta_0 = 10^{14}$ Pa s. The grey colored area in the plot represents a thermal plume in the ice shell with a temperature of 250 K (solid line), 260 K (dashes line), and 270 K (dotted line). The white area shows the ice surrounding the thermal plume with a fixed temperature 250 K.

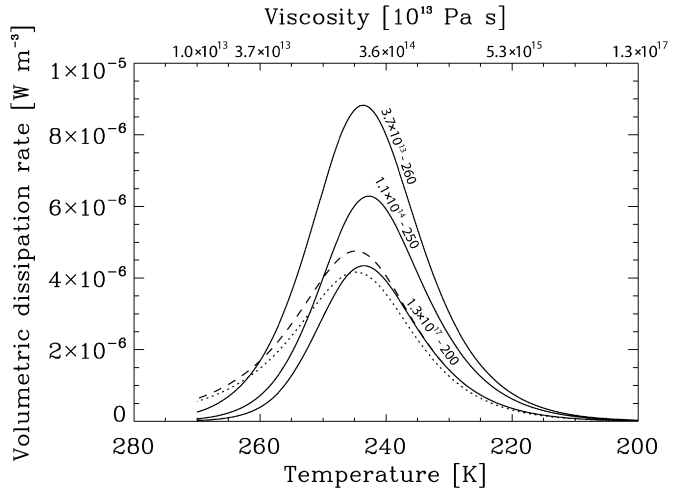

Fig. 3. Volumetric dissipation rate W in a plume of Europa versus plume temperature. The background temperature is held constant at either 200, 250, or 260 K (solid lines) for a reference viscosity is $\eta_0 = 10^{13}$ Pa s. The x-axis also shows the corresponding plume viscosity. The strain of the ice shell is 1.25×10^{-5}. The problem is solved for plane strain. The dotted line shows the volumetric dissipation rate of an incompressible zero-dimensional Maxwellian material. The dashed line shows the volumetric dissipation rate for a two-dimensional compressible Maxwellian model for a homogeneous temperature. Numbers on curves give background viscosities (in Pa s) and temperatures (in K).

perturbation in the background tidal-heating rate within several plume radii of the plume edge. Most interestingly, however, the tidal-heating rate inside the plume depends strongly on plume temperature. As expected, when the plume temperature equals the background temperature (250 K), there is no perturbation of the tidal heating rate associated with the plume, but plume temperatures warmer than the background promote increased tidal dissipation inside the plume. Note that because the dissipation as a function of temperature reaches a maximum at a

tidal flexing period $\omega^{-1} \approx \eta/\mu$, in this example we find that $W_{250\ \mathrm{K}} < W_{270\ \mathrm{K}} < W_{260\ \mathrm{K}}$.

Fig. 3 for Europa and Fig. 4 for Enceladus show the volumetric dissipation rate W in a plume versus temperature when the background temperature is held constant at either 200, 250, or 260 K (solid lines, bottom to top) when $\eta_0 = 10^{13}$ Pa s. Plane strain is assumed. On x-axis we also give the corresponding viscosity of the plume (note that the dissipation is most fundamentally a function of the plume viscosity, independent of the values of η_0 and A; it becomes a function of temperature only after η_0 and A are specified). The strain of the ice shell is fixed to 1.25×10^{-5} for Europa, and 1.0×10^{-7}, 1.0×10^{-6}, and 1.0×10^{-5} for Enceladus. This is compared with the volumetric dissipation rate of a two-dimensional compressible Maxwellian model for a homogeneous temperature (dotted line). The tidal-dissipation rate in a plume increases strongly with temperature at low temperatures and decreases with temperature at higher temperatures, reaching a maximum at intermediate temperatures. Interestingly, however, the temperature at the maximum in our solution is slightly smaller that in the zero-dimensional Maxwell model. This difference arises from the fact that the stress and strain within the plume are affected by the deformation of the surrounding matrix. We note also that an incompressible model under-estimates the effective dissipation rate (compare dotted and dashed lines of Figs. 3 and 4). Note that if $\eta_0 > 10^{14}$ Pa s then the maxima occur at temperatures above 270 K; in this case, the plume dissipation rate increases monotonically with temperature up to the melting point.

Our calculation provides the first quantitative verification of the hypothesis by Sotin et al. (2002) and others that the tidal dissipation rate is a strong function of temperature inside a convective plume.

4. Conclusions

Many authors have advanced the hypothesis that spatial localization of tidal heating occurs within convective plumes in the ice shells of Europa, Enceladus, and other icy satellites. We have tested this hypothesis using a two-dimensional compressible Maxwellian model of the deformation near and within a convective plume. The results of our model provide the first quantitative verification of the hypothesis by Sotin et al. (2002) that the tidal dissipation rate is a strong function of temperature within a convective plume, implying that spatial localization of tidal internal heating can occur within an ice shell. Our model therefore provides support for the idea that local concentration of tidal heating can promote partial melting within an ice shell (Collins et al., 2000; Sotin et al., 2002; Tobie et al., 2003). On Europa, such localized heating could help allow the formation of domes and chaos terrains by convection and/or promote resurfacing.

Schubert et al. (2007) have argued that a layer of liquid water could provide a source for the water-vapor plume spray at Enceladus' south polar region. In agreement with the considerations of Schubert et al. (2007), our results show that is quite possible that if a thermal plume or diapir exists within the ice shell, liquid water could be produced near Enceladus' surface.

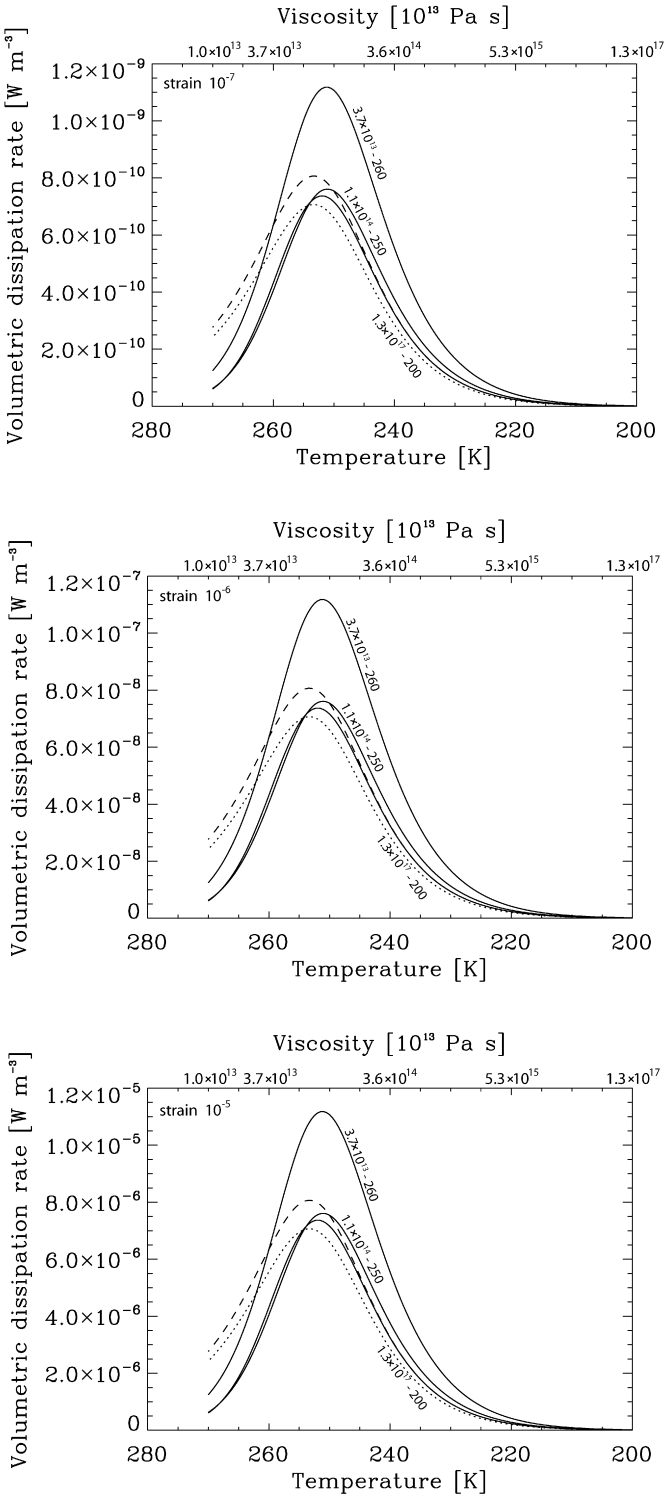

Fig. 4. Volumetric dissipation rate W in a plume of Enceladus versus plume temperature. The background temperature is held constant at either 200, 250, and 260 K (solid lines) for a reference viscosity is $\eta_0 = 10^{13}$ Pa s. The x-axis also shows the corresponding viscosity of the plume. The two panels are for strain of the ice shell 1.0×10^{-7}, 1.0×10^{-6}, and 1.0×10^{-5}. The problem is solved for plane strain. The volumetric dissipation rate of an incompressible zero-dimensional Maxwellian material is shown in dotted line. The volumetric dissipation rate for a two-dimensional compressible Maxwellian model for a homogeneous temperature is shown in dashed line. Numbers on curves give background viscosities (in Pa s) and temperatures (in K).

The presence of liquid water and high local concentration of tidal heating in the south polar region can explain the geological activity, the anomalous high temperature and heat flux, and the spray observed at the Enceladus south polar regions.

Although we focus here on Enceladus and Europa, our work may also apply to other icy bodies in the outer Solar System such as Titan, Miranda, Ariel, Triton, and Ganymede.

Acknowledgments

The authors thank Gabriel Tobie and William Moore for their careful reviews. This work was supported in part by NASA PG&G grant NNG04GI46G and NNX07AR27G to A.P.S. G.M. was supported in part by an appointment to the NASA Postdoctoral Program at the Jet Propulsion Laboratory. Part of this work was conducted at the Jet Propulsion Laboratory, California Institute of Technology, under contract with the National Aeronautics and Space Administration (NASA).

References

Biot, M.A., 1954. Theory of stress–strain relations in anisotropic viscoelasticity and relaxation phenomena. J. Appl. Phys. 25, 1385–1391.

Collins, G.C., Head, J.W., Pappalardo, R.T., Spaun, N.A., 2000. Evaluation of models for the formation of chaotic terrain on Europa. J. Geophys. Res. 105, 1709–1716.

Gaidos, E.J., Nimmo, F., 2000. Tectonics and water on Europa. Nature 405, 637.

Greenberg, R., Geissler, P., 2002. Europa's dynamic icy crust. Meteorit. Planet. Sci. 37, 1685–1710.

Greenberg, R., Hoppa, G.V., Tufts, B.R., Geissler, P., Riley, J., Kadel, S., 1999. Chaos on Europa. Icarus 141, 263–286.

Grott, M., Sohl, F., Hussmann, H., 2007. Degree-one convection and the origin of Enceladus' dichotomy. Icarus 191, 203–210.

Han, L., Showman, A.P., 2005. Thermo-compositional convection in Europa's icy shell with salinity. Geophys. Res. Lett. 32, doi:10.1029/2005GL023979. L20201.

Hetnarski, R.B., Ignaczak, J., 2004. Mathematical Theory of Elasticity. Taylor & Francis, London.

Jaeger, J.C., Cook, N.G.W., 1979. Fundamentals of Rock Mechanics, third ed. Chapman and Hall, New York.

Mal, A.K., Singh, S.J., 1991. Deformation of Elastic Solids. Prentice Hall, Englewood Cliffs, NJ.

McKinnon, W.B., 2006. On convection in ice I shells of outer Solar System bodies, with detailed application to Callisto. Icarus 183, 435–450.

Melosh, H.J., Ekholm, A.G., Showman, A.P., Lorenz, R.D., 2004. The temperature of Europa's subsurface water ocean. Icarus 168, 498–502.

Mitri, G., Showman, A.P., 2005. Convective conductive transitions and sensitivity of a convecting ice shell to perturbations in heat flux and tidal-heating rate: Implications for Europa. Icarus 177, 447–460.

Nimmo, F., Gaidos, E., 2002. Strike-slip motion and double ridge formation on Europa. J. Geophys. Res. (Planets) 107. 5-1.

Nimmo, F., Manga, M., 2002. Causes, characteristics, and consequences of convective diapirism on Europa. Geophys. Res. Lett. 29 (23), doi:10.1029/2002GL012754. 2109.

Nimmo, F., Pappalardo, R.T., 2006. Diapir-induced reorientation of Saturn's moon Enceladus. Nature 441, 614–616.

Nimmo, F., Spencer, J.R., Pappalardo, R.T., Mullen, M.E., 2007. Shear heating as the origin of the plumes and heat flux on Enceladus. Nature 447, 289–291.

Ojakangas, G.W., Stevenson, D.J., 1989. Thermal state of an ice shell on Europa. Icarus 81, 220–241.

Pappalardo, R.T., and 10 colleagues, 1998. Geological evidence for solid-state convection in Europa's ice shell. Nature 391, 365–368.

Porco, C.C., and 24 colleagues, 2006. Cassini observes the active south pole of Enceladus. Science 311, 1393–1401.

Schubert, G., Anderson, J.D., Travis, B.J., Palguta, J., 2007. Enceladus: Present internal structure and differentiation by early and long term radiogenic heating. Icarus 188, 345–355.

Showman, A.P., Han, L., 2004. Numerical simulations of convection in Europa's ice shell: Implications for surface features. J. Geophys. Res. 109 (E1), doi:10.1029/2003JE002103. E01010.

Showman, A.P., Han, L., 2005. Effects of plasticity on convection in an ice shell: Implications for Europa. Icarus 177, 425–437.

Sotin, C., Head, J.W., Tobie, G., 2002. Europa: Tidal heating of upwelling thermal plumes and the origin of lenticulae and chaos melting. Geophys. Res. Lett. 29. 74-1.

Spahn, F., and 15 colleagues, 2006. Cassini dust measurements at Enceladus and implications for the origin of the E ring. Science 311, 1416–1418.

Spencer, J.R., Pearl, J.C., Segura, M., Flasar, F.M., Mamoutkine, A., Romani, P., Buratti, B.J., Hendrix, A.R., Spilker, L.J., Lopes, R.M.C., 2006. Cassini encounters Enceladus: Background and the discovery of a south polar hot spot. Science 311, 1401–1405.

Thomson, R.E., Delaney, J.R., 2001. Evidence for a weakly stratified europan ocean sustained by seafloor heat flux. J. Geophys. Res. 106, 12355–12365.

Tobie, G., Choblet, G., Sotin, C., 2003. Tidally heated convection: Constraints on Europa's ice shell thickness. J. Geophys. Res. 108. 10-1.

Tobie, G., Mocquet, A., Sotin, C., 2005. Tidal dissipation within large icy satellites: Applications to Europa and Titan. Icarus 177, 534–549.

Waite, J.H., and 13 colleagues, 2006. Cassini Ion and Neutral Mass Spectrometer: Enceladus plume composition and structure. Science 311, 1419–1422.

Wang, H., Stevenson, D.J., 2000. Convection and internal melting of Europa's ice shell. Lunar Planet. Sci. 31. Abstract 1239.